Analyst

ROYAL SOCIETY OF CHEMISTRY

PAPER

View Article Online
View Journal

Cite this: DOI: 10.1039/d0an00673d

A dual electrochemical/colorimetric magnetic nanoparticle/peptide-based platform for the detection of *Staphylococcus aureus*

Shimaa Eissa [a] and Mohammed Zourob *[a,b]

Point-of-care facile and economical detection of *Staphylococcus aureus* (*S. aureus*), one of the main causes of food-borne illness, is highly demanded for the early diagnosis and control of infections. Herein, inspired by the proteolytic activity of *S. aureus* protease on a specific peptide substrate, we developed a rapid, simple and cost-effective biosensor for *S. aureus* using dual colorimetric and electrochemical detection on the same platform. In this approach, gold screen printed electrodes were used on which specific peptide sequences coupled to magnetic nanoparticles were immobilized giving the black color of the sensor surface. The addition of the *S. aureus* protease solution on the electrode surface causes cleavage of the peptide sequence and the release of the magnetic nanoparticles revealing the golden colour of the electrode which can be easily seen by the naked eye. Furthermore, square wave voltammetric signals can be detected on the same electrode in the ferro/ferricyanide redox couple. The change in the peak current after peptide cleavage was directly proportional to the concentration of *S. aureus*. The detection limit of the electrochemical assay was 3 CFU ml^{-1} after 1 min. Moreover, the biosensor was capable of specifically distinguishing *S. aureus* from other food- and water-borne bacteria such as *E. coli* and *Listeria* using the dual mode colorimetric and electrochemical detection. The biosensor was also tested in spiked milk and water samples showing very good recovery percentages. Thus, we believe that this dual mode biosensing platform enables the easy and accurate determination of *S. aureus* and holds great promise for point-of-care diagnosis.

Received 5th April 2020,
Accepted 18th May 2020

DOI: 10.1039/d0an00673d

rsc.li/analyst

1. Introduction

The contamination of food with bacteria represents a significant threat to public health which has been dramatically increased in the past decades. *Staphylococcus aureus* (*S. aureus*) is an anaerobic, facultative, non-spore forming Gram-positive bacterium. It is one of the most common foodborne pathogens which causes illness worldwide.[1] *S. aureus* naturally exists on mucous membranes and human skin and is able to survive in dry and hot conditions. It is considered a potential pathogen causing several types of gastrointestinal tract infections and dermatitis.[2] *S. aureus* can also produce toxins such as Staphylococcus enterotoxin that is very stable under various environmental conditions. Thus, it is considered a major threat to the food industry.[1,3]

Methicillin-resistant *Staphylococcus aureus* (MRSA) is a strain of *S. aureus* that became resistant to many antibiotics such as methicillin. Therefore, it results in many hospital-acquired and community acquired infections causing significant morbidity and mortality.[4] MRSA is usually present on the skin of animals and causes contamination of animal products such as fish, milk, meat and eggs. This can potentially harm the consumers.[5] Therefore, the detection of *S. aureus* is crucial to ensure food safety and protect public health.[3] Moreover, the detection of the contaminated food products and sites before they reach the consumers helps to avoid the infection.

Conventional cultural methods for the detection of *S. aureus* have been commonly used. However, this method is labor-intensive and time consuming as it requires 3 to 5 days to perform. Thus, more rapid detection techniques have been developed such as polymerase chain reaction (PCR) and enzyme linked immunosorbent assay (ELISA) which can be performed in several hours. However, these assays require specialized laboratories and trained personnel to perform and several incubations and washing steps which hinder their use for on-site detection. Moreover, these assays need expensive reagents which limit their widespread applications especially in developing countries with limited resources.

Therefore, there is an urgent demand to develop rapid, low-cost and portable biosensors for the easy and on-site detection

[a]Department of Chemistry, Alfaisal University, Al Zahrawi Street, Al Maather, Al Takhassusi Road, Riyadh 11533, Saudi Arabia. E-mail: mzourob@alfaisal.edu
[b]King Faisal Specialist Hospital and Research Center, Zahrawi Street, Al Maather, Riyadh 12713, Saudi Arabia

of *S. aureus*. Valuable efforts have been made in the past years for the development of various biosensors for *S. aureus*. Optical biosensors have been reported for the detection of *S. aureus* based on surface plasmon resonance,[6–9] colorimetric,[10–14] fluorescence[15–22] and surface-enhanced Raman spectroscopy techniques.[23,24] Electrochemical biosensors using potentiometric,[25,26] amperometric[27–30] and impedimetric[31–37] methods have been also reported. Various recognition receptors have been used in the fabrication of these biosensors including antibodies, aptamers, DNA, bacteriophages and peptides. However, the majority of these biosensing platforms requires complicated sensor fabrication, pretreatment step before detection and/or expensive instruments which limit their practical applications.

Colorimetric- and electrochemical-based biosensors have received special attention in recent years exhibiting significant capability to detect bacteria in various matrices. Colorimetric biosensors enable simple naked-eye readout without complex instruments, thus possessing potential for on-site screening. However, colorimetric biosensors often provide a "yes" or "no" answer or relatively poor quantitative detection which restricts their useful applications for sensitive bacteria detection. Therefore, much effort has been directed toward electrochemical biosensors for the quantification of bacteria as the most promising approach for sensitive, low-cost, rapid, easy and automated detection.

Some strip format paper-based biosensors have been recently developed for bacteria detection exploiting the capability of the bacteria to produce protease.[38] Using this approach, a colorimetric biosensor for *S. aureus* was reported[14] that utilises a specific peptide sequence for *S. aureus* immobilized on a gold coated paper. The protease was used as a biomarker that indicates the presence of the *S. aureus* bacteria in a very short time. However, this colorimetric method is yet constrained by the sample background colour and therefore, sometimes does not satisfy current needs for accurate and sensitive bacteria detection.

In this study, we aim to combine the advantages of colorimetric detection for screening and electrochemical detection for the accurate quantitative analysis of *S. aureus*. The objective of this work is to use a peptide/magnetic bead probe on a screen printed electrode (SPE) to detect *S. aureus* protease *via* a dual electrochemical/colorimetric detection. The specific *S. aureus* peptide coupled to black magnetic nanoparticles is immobilised on a gold screen printed electrode. The presence of the *S. aureus* protease on the biosensor surface causes a cleavage of the peptide and the release of the magnetic beads from the surface. This can be detected by visualising the change of the working electrode color from black to golden yellow as well as by monitoring the change in the square wave voltammetric peak current after only 1 min. By applying this dual detection technique, a simple, fast, cost-effective biosensor was developed. Compared with the available electrochemical and colorimetric biosensors for *S. aureus*, our method is much faster and easier to perform without complex sample processing steps. Unlike other electrochemical biosensors, this method does not employ enzymes as the detection probe avoiding the need for several steps and long analysis time as well as enzyme instability. Moreover, a visible color change which reflects the bacterial concentration can be observed by the naked eye on the same electrode platform.

2. Experimental section

2.1. Materials and reagents

Disposable gold screen printed electrodes (SPE) were purchased from DropSens, Inc. (Spain, ref. 220 AT). Each electrode contains a 4 mm diameter working electrode prepared from gold with high temperature curing ink, a gold counter electrode and silver reference electrodes. All the electrical contacts are made of silver. Carboxylate-modified magnetic nanobeads (around 50 nm in diameter) were obtained from TurboBeads (Zurich, Switzerland). The *S. aureus* biotinylated peptide sequence (NH_2-Ahx-ETKVEENEAIQK Ahx-biotin) was synthesised by Pepmic Co., Ltd (Suzhou, China). Streptavidin, bovine serum albumin (BSA), ethanol amine, *N*-hydroxysuccinimide (NHS), 1-(3-dimethylaminopropyl)-3-ethyl-carbodiimide (EDC), potassium ferrocyanide ($K_4Fe(CN)_6$), potassium ferricyanide ($K_3Fe(CN)_6$), dipotassium hydrogen orthophosphate, sodium chloride and potassium dihydrogen orthophosphate were purchased from Sigma Aldrich (Ontario, Canada). Sterile filters, 0.22 μm were obtained from EMD Millipore (Alberta, Canada). Brain heart infusion (BHI) agar and broth were obtained from SDA Oxoid, Ltd (Basingstoke, UK). A phosphate buffered saline (PBS) solution (10 mM, pH 7.4) was used to dissolve the 1 : 1 redox couple $[Fe(CN)_6]^{4-/3-}$. The peptide stock solution was prepared in DMSO and diluted using PBS buffer, pH 7.4. PBS buffer, pH 5.5 was used to dissolve the EDC/NHS for the magnetic nanoparticles activation step. Aqueous solution of ethanol amine, pH, 8.0 was used to block the free carboxylic sites on the beads. 1% BSA was prepared in PBS buffer, pH 7.4. All the solutions were prepared in Milli-Q grade water.

2.2. Instrumentation

All the electrochemical measurements (cyclic and square wave voltammetry) were performed using an Autolab PGSTAT302N potentiostat (Eco Chemie, The Netherlands). The potentiostat is connected to a computer and operated by 1.11 NOVA software. The screen printed electrodes were connected to the potentiostat using a connector obtained from DropSens (Spain).

2.3. Methods

2.3.1. Preparation of bacterial culture and the extraction of protease. *S. aureus* (ATCC 25923), *E. coli* O157:H7 and *Listeria* monocytogenes (ATCC 19115) were purchased from Sigma Aldrich (UK). Each bacteria strain was streaked on BHI agar plate and incubated at 37.0 °C for 24 h. After incubation, one colony from each bacterial strain was then picked up and inoculated into BHI broth overnight at 37 °C. The primary bac-

terial culture (PBC) was serially diluted for counting. The bacterial colony forming unit (CFU mL^{-1}) values of the different cultures were determined using the viable count spread dilution method. The serial dilutions of each bacterial culture were centrifuged at 3000×*g* for 10 min until cell pellets were obtained. The supernatants were then separated from the pellets and filtered using 0.22 μm pore size-syringe filters to obtain the pure enzyme solution. In order to confirm that the protease proteolytic activity is correlated to the concentration of the *S. aureus* bacteria, the enzyme activity was determined using the universal casein assay *via* measuring the number of micromoles of tyrosine equivalents released from casein per minute.[39] The quantification of the protease activity and its correlation to the concentration of *S. aureus* have been reported in previous work.[14]

2.3.2. Immobilization of *S. aureus* peptide on the magnetic nanobeads. The carboxylated magnetic nanobeads were activated using EDC/NHS. 10 mg of beads were washed several times with PBS buffer, pH 5.5 then mixed with 40 mg of EDC and 15 mg of NHS in 500 μl of PBS buffer, pH 5.5. The mixture was incubated at room temperature with end-over-end rotation for 1 h. After mixing, the excess EDC and NHS solution was removed by washing the beads with PBS buffer, pH 7.4. The activated beads were then incubated with 1 mg ml^{-1} of biotinylated *S. aureus* peptide in PBS buffer pH 7.4 and mixed at room temperature with end-over-end rotation. After that, the beads were washed with PBS buffer pH 7.4 several times. The unreacted carboxylic groups on the magnetic beads were then blocked by incubation with 0.1 M ethanol amine solution pH 8.0. Then, the magnetic beads were washed again with PBS buffer and kept in 500 μl of the same buffer.

2.3.3. Preparation of the *S. aureus* biosensor on gold screen printed electrodes. The attachment steps of the magnetic nanobead/peptide conjugate to the gold electrode surface are shown in the scheme (Fig. 1). First, the gold electrodes were coated with streptavidin. 20 μl of 10 μg ml^{-1} streptavidin solution in PBS buffer pH 7.4 was placed on the gold working electrode of the SPE and incubated for 1 h at 37 °C. After incubation, the electrodes were washed with PBS buffer to remove the excess streptavidin. Second, 20 μl of the peptide-modified magnetic beads were placed on the streptavidin coated gold electrode surface and kept at 37 °C for 1 h. The magnetic bead/peptide modified electrodes (black color) were then washed with PBS buffer and used as a biosensor for

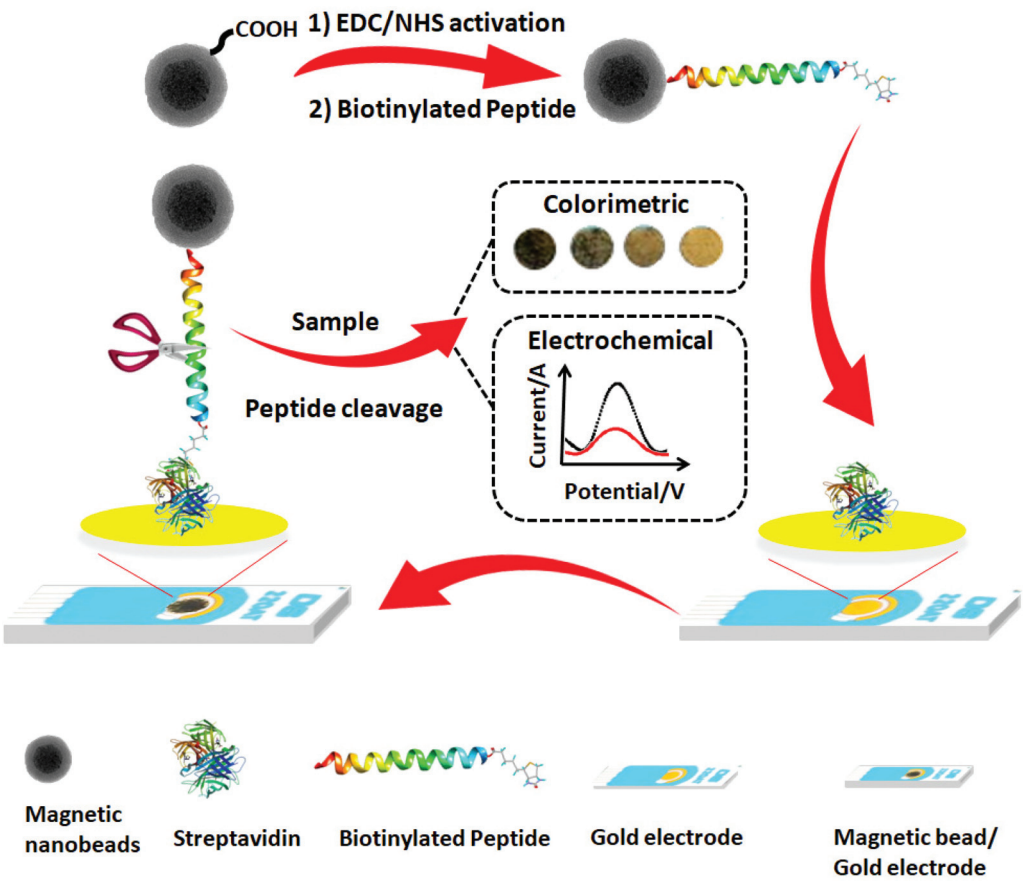

Fig. 1 Scheme of the peptide/magnetic bead biosensor for *Staphylococcus aureus* using dual electrochemical and colorimetric detection on screen printed gold electrodes. The activation of the biotinylated peptide on the magnetic beads was done using EDC/NHS chemistry. The biotinylated peptide-modified beads were then attached to the streptavidin coated screen printed carbon electrodes. Electrochemical and colorimetric detection were used to monitor the cleavage of the peptide by the bacteria protease.

S. aureus detection. The excess magnetic beads can be also removed by placing a magnet over the working electrode area. The formation of a black layer on the working electrode area compared with the golden yellow color of the streptavidin coated electrode (as shown in Fig. 1) indicates the success of the immobilization of the peptide/magnetic beads on the electrode surface. The biosensors were used immediately or stored dried at 4 °C until further use. The characterization of the immobilization steps was carried out using cyclic voltammetry (CV) scans at a scan rate of 100 mV s^{-1} within a potential range of −0.2 to 0.45 V as well as square wave voltammetry (SWV) in 5 mM ferro/ferricyanide redox solution.

2.3.4. Colorimetric detection of *S. aureus* bacteria. 20 μl of the protease solutions from *S. aureus* bacterial culture (from 10^1 to 10^8 CFU ml^{-1}) were placed on the *S. aureus* biosensors and incubated for 1 min. After that, the cleaved peptide/magnetic beads were removed from the electrode surface by washing with PBS buffer pH 7.4 or by moving a magnet under the working electrode area towards the electrical contact. Upon removal of some magnetic nanobeads from the surface due to the peptide cleavage by the protease, the colour of the working electrode gradually changes from black to golden yellow. The decrease in the intensity of the black colour can be visualised by the naked eye or captured with a smart phone.

2.3.5. Electrochemical detection of *S. aureus*. After incubation of the bacterial protease solution on the electrodes for 1 min and visualising the colour change, the SWV measurements were performed by placing 100 μl of 5 mM ferro/ferricyanide redox solution in PBS buffer on the SPE in such a way to cover the three electrodes. The SWV measurements were recorded at a scan rate of 125 mV s^{-1}, amplitude = 20 mV, interval time = 0.04 s, frequency = 25 Hz, step potential = −5 mV. The detection was achieved *via* following the change in the reduction peak current of the redox couple before and after the peptide cleavage $(i - °)/i°\%$, where $i°$ is the peak current of the biosensor before incubation with the protease and i is the peak current after incubation with different concentrations of bacteria supernatant containing protease.

2.3.6. Optimization of the incubation time of the protease solution on the magnetic bead/peptide biosensor. The protease solution from 10^3 CFU ml^{-1} *S. aureus* culture was incubated on the biosensor for different time intervals (0.25, 0.5, 1, 5 and 10 min). The electrodes were washed after each incubation period and the SWV measurements were recorded following the protocol described above.

2.3.7. Study of the cross reactivity of the *S. aureus* biosensor with nonspecific bacteria. Different protease solutions extracted from different bacteria strains (*Listeria* and *E. coli*) were prepared as described above. 20 μl of each protease solution (from 10^3 CFU ml^{-1} of bacteria) were incubated on separate sensors for 1 min at room temperature. Then, the cleaved peptide-magnetic beads were removed from the electrode surface with a magnet. The colour change was then visualized in each case. Then, SWV scans were recorded in each case before and after incubation with the specific and nonspecific bacteria protease. The responses to the various bacteria types were compared by monitoring the percentage change in the reduction peak current after cleavage.

2.3.8. Application of the *S. aureus* biosensor in spiked water and milk samples. Full milk and bottled water samples obtained from a local store in Riyadh city were used for testing. 1 ml of milk was centrifuged at 4000*g* for 10 min and the supernatant was filtered using 0.22 μm syringe filters. The sample was spiked with 10^3 CFU ml^{-1} *S. aureus* bacterial supernatant and then diluted 1 : 10 in PBS buffer pH 7.4. 1 ml of water was spiked with 10^3 CFU ml^{-1} *S. aureus* bacterial supernatant and then added to 9 ml of PBS buffer pH 7.4. Non spiked samples were used as negative controls to check the effect of the food matrix on the biosensor output.

20 μl of each spiked sample were then added to the surface of the working electrodes and the color change was visualized by the naked eye. Then, the ferro/ferricyanide redox solution was added and SWV measurements were recorded as described above.

3. Results and discussion

3.1. The working principle of the *S. aureus* biosensor using dual colorimetric and electrochemical detection

Various types of bacteria secrete different proteases in order to breakdown the peptide bonds in proteins to smaller polypeptides or single amino acids through hydrolysis reactions. Bacterial proteases are highly important for the digestion of ingested proteins, recycling process of the protein and maintaining the global nitrogen and carbon cycles. Some of the bacterial proteases are highly specific and only cleave substrates with a certain sequence. Upon selecting the peptide sequence that shows a high degree of proteolysis when exposed to certain bacterial protease, it can be used as a specific substrate for the enzyme.

The current biosensor is based on a peptide sequence (ETKVEENEAIQK) which was previously selected and showed specificity for *S. aureus* protease.[14,40] This peptide can be cleaved at a specific cleavage site by the *S. aureus* protease. In order to elongate the sequence to avoid steric hindrance and to have a suitable access for the protease to the cleavage site, Ahx linker is used as a spacer. The peptide is modified with the biotin molecule from the C terminal to enable the binding of the peptide to a streptavidin coated gold electrode. However, the other N-terminal of the peptide sequence is coupled to carboxylated carbon-coated magnetic nanoparticles *via* EDC/NHS chemistry. The immobilization of the magnetic nanoparticle/peptide probe on the SPE causes the formation of a black layer on the gold electrode surface. Upon the addition of the bacterial protease solution on the sensor surface the peptide is cleaved leading to the dissociation of the magnetic nanoparticles from the electrode surface which can be detected visually by color change and electrochemically by measuring the change in the SWV signal as shown in the scheme (Fig. 1).

3.2. Characterization of the fabrication steps of the *S. aureus* peptide/magnetic bead sensor

First, to prepare the magnetic bead/peptide probe, a biotinylated peptide and carboxylate magnetic nanobeads were used. The beads were activated using EDC/NHS chemistry and then incubated with the biotinylated peptide. The N-terminal of the peptide sequence binds to the bead *via* the amide covalent bond leaving the biotinylated end free.

Second, gold SPEs were coated with streptavidin protein to enable the attachment of the biotinylated peptide/magnetic bead probe to the gold surface *via* the very strong non covalent biotin–streptavidin binding.

CV and SWV techniques were used for the characterization of the modification steps of the electrodes. Fig. 2A and B show the CV and the SWV measured in ferro/ferricyanide redox solution of the bare gold electrode, the streptavidin-modified electrode, after blocking the surface with BSA and after the immobilization of the biotinylated peptide/magnetic bead probe. As shown in Fig. 1A, the bare gold electrode showed the reversible characteristic peaks of the clean gold surface with a peak-to-peak separation (ΔE) of around 100 mV indicating the fast electron transfer process on the highly conductive gold. After the adsorption of the streptavidin on the gold surface, the anodic and cathodic peaks in the CV were decreased and the ΔE slightly increased. This is attributed to the coverage of the gold with the protein which retards the electron transfer. It is worth mentioning that the streptavidin protein is neutral at pH 7.4, thus, there is almost no effect of its electrostatic charge on the voltammetric signal. The blocking of the free gold surface with BSA caused a further decrease in the current and increase in the ΔE due to the bulky size of the BSA. The binding of the biotinylated peptide/magnetic bead probe to the streptavidin coated surface resulted in a dramatic decrease in the anodic and cathodic peaks and an increase in the ΔE. The magnetic beads consist of metallic nanoparticles coated with a thin (2 nm) graphene-like carbon layer. The attachment of the carbon-coated nanoparticles caused a retardation of the electron transfer process and thus, a decrease in the current and an increase in the ΔE. These results were also confirmed using SWV measurements for each step. As shown in Fig. 2B, the SWV reduction peak of the ferro/ferricyanide redox couple was gradually decreasing after each modification step indicating the formation of the streptavidin layer, the blocking with BSA and the attachment of the peptide/magnetic nanoparticle probe. On the other hand, the addition of *S. aureus* protease from 10^8 CFU ml^{-1} bacteria culture caused a significant increase in the SWV reduction peak current due to the cleavage of the peptide sequence which links the magnetic nanoparticles to the gold surface. This leads to the removal of the magnetic particles from the electrode surface and thus, the enhancement of the electron transfer process leading to an increase in the peak current. The increase of the SWV peak current upon the addition of the bacteria protease due to the peptide cleavage represents the basis of the electrochemical detection.

3.3. Optimisation of the time of the *S. aureus* bacteria detection on the peptide/magnetic particle biosensor

The reduction of the time needed for detection is critical in the development of a biosensor for field applications. In order to gain insight into the effect of the incubation period of the bacteria protease solution on the peptide sensor surface, the biosensor was incubated with *S. aureus* protease from 10^2 CFU ml^{-1} bacterial cultures for different time intervals. Fig. 3A, shows the biosensor response, measured as the percentage change of the SWV reduction peak current, after the addition of the protease solution on the electrode surface for different incubation periods (from 0.25 to 10 min). As shown in the

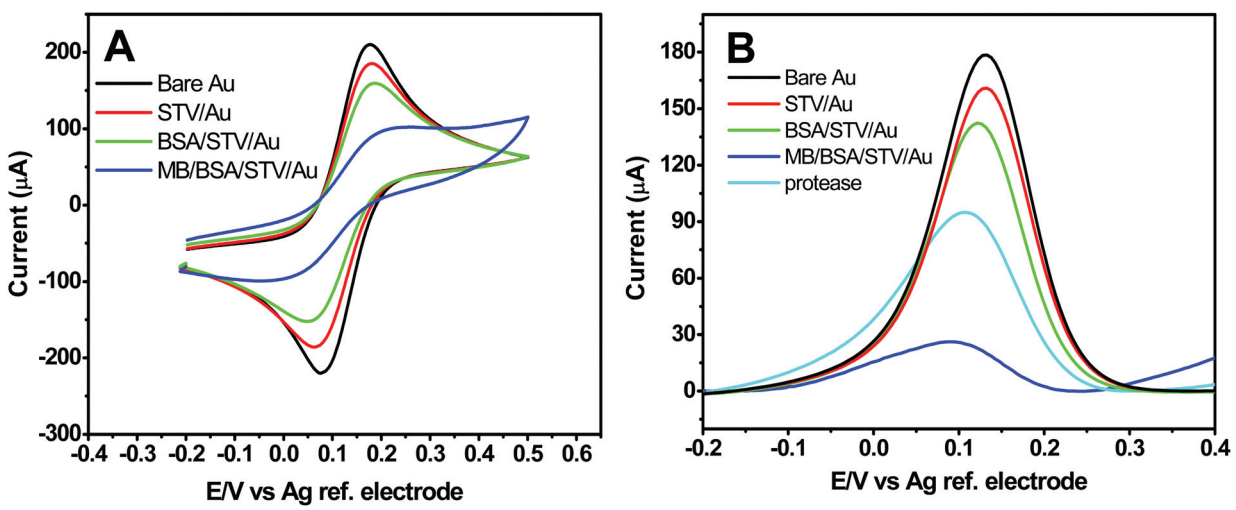

Fig. 2 Cyclic voltammetry (A) and square wave voltammetry (B) of 5 mM $[Fe(CN)_6]^{4-/3-}$ redox solution in PBS buffer, pH 7.4, for the bare gold screen printed electrode (black), streptavidin coated electrodes (red), magnetic bead/peptide modified electrode (green), BSA blocked electrode (blue) and after adding the protease of *S. aureus* bacteria (cyan). The scan rate of the cyclic voltammetry measurements was 100 mV s^{-1}. The SWV was recorded using an amplitude of 0.1 mV, a scan rate of 125 mV s^{-1}, interval time: 0.04 s, frequency: 25 Hz, and step potential: 0.01 V.

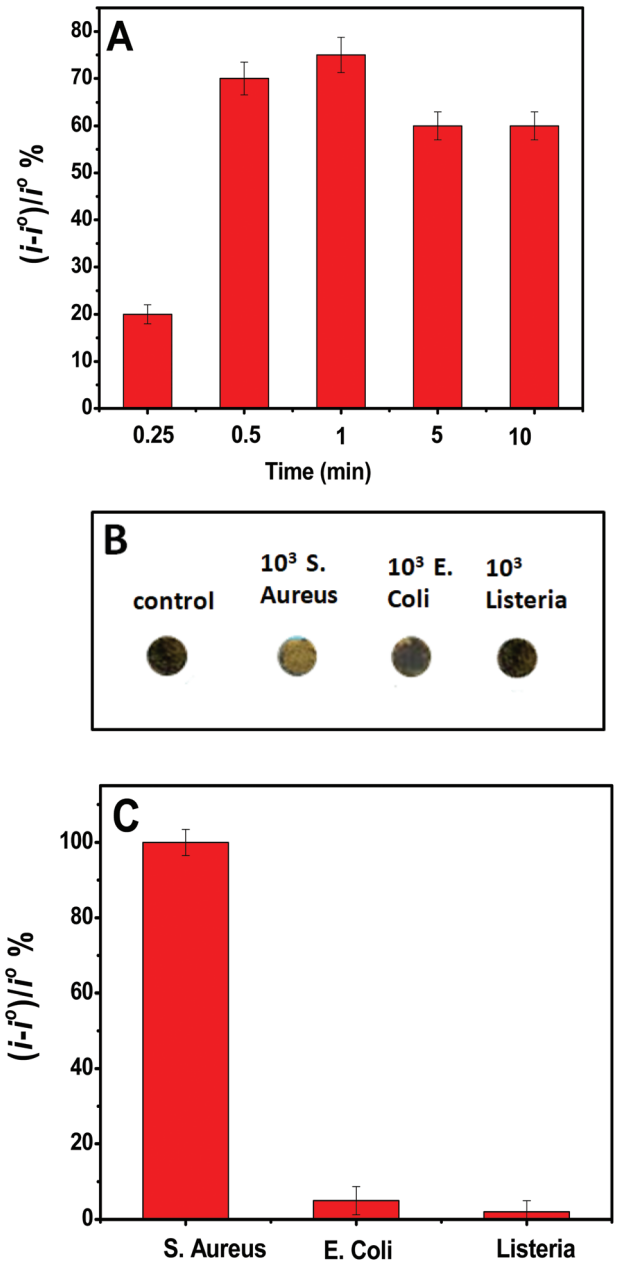

Fig. 3 Effect of incubation time of the protease of 10^2 CFU ml^{-1} bacterial culture on the magnetic bead/peptide-modified electrode (A). Colorimetric response (the images of the working electrode area) to different types of bacteria proteases (*S. aureus*, *Listeria* and *E. coli*) after 1 min incubation on the sensor surface (B). Electrochemical response (the percentage change in the SWV reduction peak current ($i - i°$)/$i°$%) after incubation of different bacteria protease on the sensor surface (C), where i is the peak current after protease incubation and $i°$ is the peak current of the sensor (the magnetic bead/peptide-modified electrode). The error bars represent the standard deviations of duplicate measurements.

figure, the *S. aureus* biosensor response increased with increasing incubation period. After 15 s, the sensor response was around 20% and then significantly increased (70 to 75%) after the addition of the protease for 0.5 to 1 min indicating the fast proteolytic activity of the protease on the peptide substrate within a minute. However, the incubation of the protease solution on the biosensor for a longer period (5 to 10 min) caused a decrease in the sensor response. This is likely attributed to the nonspecific adsorption of the protease on the electrode surface at longer incubation periods which results in the shielding of the surface and diminishing of the electron transfer process. Therefore, the optimum read out time of the biosensor was chosen to be after one min of protease incubation.

3.4. Selectivity testing of the biosensor with other bacteria using colorimetric and electrochemical detection

In order to evaluate the capability of the biosensor to distinguish between different types of bacteria, protease solutions from 10^3 CFU ml^{-1} of *E. coli*, *S. aureus* and *Listeria* were tested on the biosensor surface. These bacteria are considered common food and water contaminants. Fig. 3B shows the colorimetric response on the working electrode area after incubating the sensor with the various protease solutions. After 1 min of incubation, the color of the electrode changes showing a decrease in the intensity of the black color and an appearance of the golden yellow colour only in the case of the *S. aureus* protease solution. However, there was no change observed in the black colour of the electrodes after incubation with *E. coli* and *Listeria* proteases. Fig. 3C shows the voltammetric response of the biosensor to the different types of bacteria. The electrochemical response (($i - i°$)/$i°$%) was remarkable only in the case of *S. aureus*, whereas no significant response was observed for *E. coli* and *Listeria*. These results imply the capability of the biosensor to identify *S. aureus* from other common bacteria that contaminate food and water both colorimetrically and electrochemically.

3.5. Detection of different concentrations of *S. aureus* bacteria on the peptide/magnetic particle biosensor

In order to assess the analytical range of the biosensor, various protease solutions from different concentrations of *S. aureus* ranging from 10 to 10^8 CFU ml^{-1} were tested. As shown in Fig. 4A, the images of the working electrode area showed an obvious color gradient (a decrease in the intensity of the black colour and the appearance of the golden colour) upon incubation with various protease solutions with increased concentrations of *S. aureus* bacteria. The proportional increase in the golden yellow color of the electrode is due to the proteolytic activity of the *S. aureus* protease which cleaves the peptide leading to the dissociation of the magnetic particles from the gold electrode surface. A control sample represents the biosensor before applying any protease solution and after adding PBS buffer, pH 7.4. The control did not show any color change indicating that the change in the colour appears only after adding the specific protease samples. As shown in the figure, the change in the colour can be easily seen with the naked eye from 10^2 to 10^8 CFU ml^{-1} or captured by a smart phone for colorimetric analysis.

To quantify the electrochemical response of the biosensor, SWV measurements were recorded in ferro/ferricyanide redox solution. Fig. 4B shows the SWV reduction peaks before and

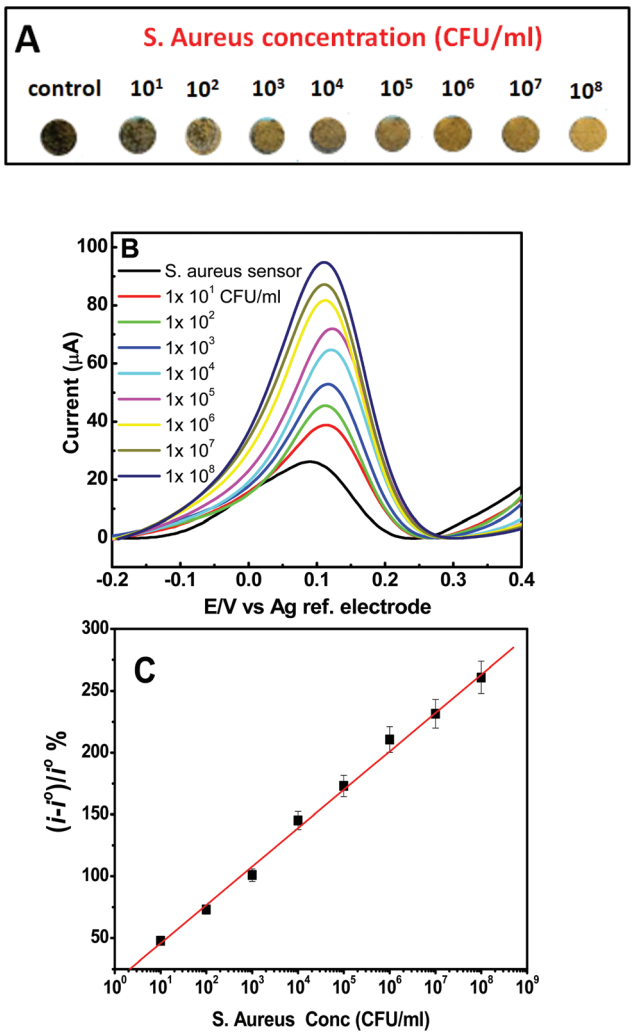

Fig. 4 Colorimetric (A) (the colour change of the working electrode from black to golden yellow) and electrochemical response (B) (the change in the SWV reduction peaks) upon incubation of the sensor with protease solution with different concentrations of *S. aureus* bacteria culture (10 to 1 × 10^8 CFU ml^{-1}). (C) The calibration plot for *S. aureus* detection (a plot of $(i - i°)/i°\%$ *versus* the concentration of bacteria culture. The error bars represent the standard deviation of duplicate measurements.

after incubation of the sensor with the protease from different concentrations of *S. aureus* bacteria (10–10^8 CFU ml^{-1}). The reduction peak current gradually increased with increasing bacteria concentration due to the cleavage of the peptide by the protease as explained above. This dissociation of the peptide/magnetic particle from the surface leads to better access of the redox molecules to the gold surface. Consequently, this quickens the electron transfer process which results in an increase in the reduction current. Fig. 4C shows the electrochemical calibration plot of the *S. aureus* sensor (a plot of the biosensor response $((i - i°)/i°\%)$ *versus* the bacteria concentration). A linear response of the peptide/magnetic bead biosensor was obtained from 10 to 10^8 CFU ml^{-1} of *S. aureus*. The limit of detection (LOD) of the biosensor

Table 1 Application of the biosensor of *S. aureus* in spiked water and milk samples using colorimetric and electrochemical detection. The relative standard deviations of 2 measurements are shown

	Electrochemical			
Sample	Found concentration	Recovery (%)	RSD (%)	Colorimetric
Spiked milk (10^3 CFU ml^{-1})	1.2 × 10^3	102	6.5	Control Sample
Spiked water (10^3 CFU ml^{-1})	9.8 × 10^2	98	4.4	Control Sample

was 3 CFU ml^{-1}, calculated as the concentration of the bacteria which results in a response equal to three times the standard deviation of the blank sample. The linear regression equation of the calibration plot is: $(i - i°)/i°\% = 14.7 + 31.05 \log C$ [CFU ml^{-1}], $R = 0.997$. The relative standard deviations of the measurements ranged from 4.0 to 6.0% indicating excellent reproducibility. This LOD is lower than the LOD of the majority of the previously reported electrochemical biosensors. Moreover, unlike the reported electrochemical sensors based on antibodies and aptamers which require a minimum of 30 min to 1 h to perform, our biosensor takes only 1 min to obtain the results.

3.6. Application of the biosensor on spiked milk and water samples

The developed peptide/magnetic nanoparticle biosensor was then examined in milk and tap water samples. The two samples were spiked with 10^3 CFU ml^{-1} *S. aureus* protease and applied on the biosensor surface. As shown in Table 1, the colour change observed in both cases was comparable with the change seen in PBS buffer. Moreover, the electrochemical measurements showed very good recovery percentages in both cases ranging from 98 to 102% with a standard deviation of 6.5 and 4.4 for the milk and water samples, respectively. These results indicate that there is no remarkable sample matrix effect on the colorimetric and electrochemical biosensor response signals, and thus, the biosensor can be applied for the detection of *S. aureus* in real food samples.

4. Conclusion

In this work, we developed for the first time a dual-mode biosensor platform for the detection of *S. aureus* based on bacteria protease activity on a specific peptide substrate coupled to magnetic nanoparticles. The detection mechanism was based on the cleavage of the peptide sandwiched between a gold electrode surface and magnetic nanoparticle by the *S. aureus* protease. The cleavage leads to the dissociation of the black magnetic particles from the biosensor surface. This release results in a decrease in the intensity of the black colour

of the electrode surface and the appearance of golden colour that can be seen by the naked eye. More sensitive and accurate detection was also recorded on the same platform by following the change in the electrochemical signal due to the release of the magnetic particles. The biosensor showed very good sensitivity for *S. aureus* in 1 min as well as excellent selectivity against other bacteria that commonly contaminate food stuff such as *E. coli* and *Listeria*. The biosensor was also applied in spiked milk and water samples showing good recovery percentages. Our biosensor combines the high sensitivity of electrochemical detection and the simplicity of colorimetric screening making it a rapid, simple and excellent tool for the on-site monitoring of *S. aureus* in food and water samples.

Conflicts of interest

The authors declare that there is no conflict of interest.

Acknowledgements

The authors would like to thank King Abdulaziz City for Science and Technology (KACST) for the financial support of this work. The authors would like to thank Ms. Duha Fawzi Saad for preparing the bacterial culture.

References

1 M. Rubab, H. M. Shahbaz, A. N. Olaimat and D.-H. Oh, *Biosens. Bioelectron.*, 2018, **105**, 49–57.
2 J. Kadariya, T. C. Smith and D. Thapaliya, *BioMed Res. Int.*, 2014, **2014**, 827965–827965.
3 S. Y. C. Tong, J. S. Davis, E. Eichenberger, T. L. Holland and V. G. Fowler Jr., *Clin. Microbiol. Rev.*, 2015, **28**, 603–661.
4 R. Adhikari, N. D. Pant, S. Neupane, M. Neupane, R. Bhattarai, S. Bhatta, R. Chaudhary and B. Lekhak, *Can. J. Infect. Dis. Med. Microbiol.*, 2017, **2017**, 2191532–2191532.
5 H. Yang, X. Ma, X. Zhang, Y. Wang and W. Zhang, *Eur. Food Res. Technol.*, 2011, **232**, 769–776.
6 S. Balasubramanian, I. B. Sorokulova, V. J. Vodyanoy and A. L. Simonian, *Biosens. Bioelectron.*, 2007, **22**, 948–955.
7 L. Chen, L. Deng, L. Liu and Z. Peng, *Biosens. Bioelectron.*, 2007, **22**, 1487–1492.
8 N. Tawil, E. Sacher, R. Mandeville and M. Meunier, *Biosens. Bioelectron.*, 2012, **37**, 24–29.
9 N. Tawil, F. Mouawad, S. Lévesque, E. Sacher, R. Mandeville and M. Meunier, *Biosens. Bioelectron.*, 2013, **49**, 334–340.
10 P. Liu, L. Han, F. Wang, V. A. Petrenko and A. Liu, *Biosens. Bioelectron.*, 2016, **82**, 195–203.
11 C.-Z. Li, K. Vandenberg, S. Prabhulkar, X. Zhu, L. Schneper, K. Methee, C. J. Rosser and E. Almeide, *Biosens. Bioelectron.*, 2011, **26**, 4342–4348.
12 J. Yuan, S. Wu, N. Duan, X. Ma, Y. Xia, J. Chen, Z. Ding and Z. Wang, *Talanta*, 2014, **127**, 163–168.
13 Y. J. Sung, H.-J. Suk, H. Y. Sung, T. Li, H. Poo and M.-G. Kim, *Biosens. Bioelectron.*, 2013, **43**, 432–439.
14 G. A. R. Y. Suaifan, S. Alhogail and M. Zourob, *Biosens. Bioelectron.*, 2017, **90**, 230–237.
15 H. N. Abdelhamid and H.-F. Wu, *J. Mater. Chem. B*, 2013, **1**, 3950–3961.
16 X. Xue, J. Pan, H. Xie, J. Wang and S. Zhang, *Talanta*, 2009, **77**, 1808–1813.
17 P. Zuo, X. Li, D. C. Dominguez and B.-C. Ye, *Lab Chip*, 2013, **13**, 3921–3928.
18 T. Miao, Z. Wang, S. Li and X. Wang, *Microchim. Acta*, 2011, **172**, 431–437.
19 J. Shangguan, Y. Li, D. He, X. He, K. Wang, Z. Zou and H. Shi, *Analyst*, 2015, **140**, 4489–4497.
20 N. Duan, S. Wu, C. Zhu, X. Ma, Z. Wang, Y. Yu and Y. Jiang, *Anal. Chim. Acta*, 2012, **723**, 1–6.
21 S. Wu, N. Duan, Z. Shi, C. Fang and Z. Wang, *Anal. Chem.*, 2014, **86**, 3100–3107.
22 X. Wang, Y. Du, Y. Li, D. Li and R. Sun, *J. Biomater. Sci., Polym. Ed.*, 2011, **22**, 1881–1893.
23 H. Zhang, X. Ma, Y. Liu, N. Duan, S. Wu, Z. Wang and B. Xu, *Biosens. Bioelectron.*, 2015, **74**, 872–877.
24 J. Wang, X. Wu, C. Wang, N. Shao, P. Dong, R. Xiao and S. Wang, *ACS Appl. Mater. Interfaces*, 2015, **7**, 20919–20929.
25 G. A. Zelada-Guillén, J. L. Sebastián-Avila, P. Blondeau, J. Riu and F. X. Rius, *Biosens. Bioelectron.*, 2012, **31**, 226–232.
26 R. Hernández, C. Vallés, A. M. Benito, W. K. Maser, F. Xavier Rius and J. Riu, *Biosens. Bioelectron.*, 2014, **54**, 553–557.
27 L. Xu, W. Liang, Y. Wen, L. Wang, X. Yang, S. Ren, N. Jia, X. Zuo and G. Liu, *Biosens. Bioelectron.*, 2018, **99**, 424–430.
28 V. Escamilla-Gómez, S. Campuzano, M. Pedrero and J. M. Pingarrón, *Talanta*, 2008, **77**, 876–881.
29 V. Escamilla-Gómez, S. Campuzano, M. Pedrero and J. M. Pingarrón, *Anal. Bioanal. Chem.*, 2008, **391**, 837.
30 V. Escamilla-Gómez, S. Campuzano, M. Pedrero and J. M. Pingarrón, *Electroanalysis*, 2007, **19**, 1476–1482.
31 X. Tang, D. Flandre, J.-P. Raskin, Y. Nizet, L. Moreno-Hagelsieb, R. Pampin and L. A. Francis, *Sens. Actuators, B*, 2011, **156**, 578–587.
32 F. Tan, P. H. M. Leung, Z.-B. Liu, Y. Zhang, L. Xiao, W. Ye, X. Zhang, L. Yi and M. Yang, *Sens. Actuators, B*, 2011, **159**, 328–335.
33 M. Braiek, K. B. Rokbani, A. Chrouda, B. Mrabet, A. Bakhrouf, A. Maaref and N. Jaffrezic-Renault, *Biosensors*, 2012, **2**, 417–426.
34 K. Bekir, H. Barhoumi, M. Braiek, A. Chrouda, N. Zine, N. Abid, A. Maaref, A. Bakhrouf, H. B. Ouada, N. Jaffrezic-Renault and H. B. Mansour, *Environ. Sci. Pollut. Res.*, 2015, **22**, 15796–15803.

35 F. Jia, N. Duan, S. Wu, X. Ma, Y. Xia, Z. Wang and X. Wei, *Microchim. Acta*, 2014, **181**, 967–974.
36 X. Liu, M. Marrakchi, D. Xu, H. Dong and S. Andreescu, *Biosens. Bioelectron.*, 2016, **80**, 9–16.
37 A. C. Ward, A. J. Hannah, S. L. Kendrick, N. P. Tucker, G. MacGregor and P. Connolly, *Biosens. Bioelectron.*, 2018, **110**, 65–70.
38 S. Wignarajah, G. A. R. Y. Suaifan, S. Bizzarro, F. J. Bikker, W. E. Kaman and M. Zourob, *Anal. Chem.*, 2015, **87**, 12161–12168.
39 C. Cupp-Enyard, *J. Vis. Exp.*, 2008, 899.
40 M. C. Sanders, G. J. Colpas, D. L. Ellis-Busby and J. M. Havard, Google Patent, WIPO (PCT), WO2005042771A2, 2005.